INDIAN JOURNAL OF SCIENCE AND TECHNOLOGY

RESEARCH ARTICLE

Classification of Liver Lesion Stages using pyRadiomics Features Combined with 3D-CNN in 3D-CT and US Images

A Bathsheba Parimala[1]*, R S Shanmugasundaram[2]

1 Research Scholar, Department of Computer Science and Engineering, Vinayaka Mission's Kirupananda Variyar Engineering College (A Constituent College of Vinayaka Mission's Research Foundation (Deemed to be University)), Salem, 636308, Tamil Nadu, India
2 Professor, Department of Computer Science and Engineering, Vinayaka Mission's Kirupananda Variyar Engineering College (A Constituent College of Vinayaka Mission's Research Foundation (Deemed to be University)), Salem, 636308, Tamil Nadu, India

OPEN ACCESS

Received: 08-07-2024

Accepted: 08-10-2024

Published: 12-11-2024

Citation: Parimala AB, Shanmugasundaram RS (2024) Classification of Liver Lesion Stages using pyRadiomics Features Combined with 3D-CNN in 3D-CT and US Images . Indian Journal of Science and Technology 17(41): 4296-4306. https://doi.org/10.17485/IJST/v17i41.2212

* **Corresponding author**.

bathshebajournal@yahoo.com

Funding: None

Competing Interests: None

Published By Indian Society for Education and Environment (iSee)

ISSN
Print: 0974-6846
Electronic: 0974-5645

Abstract

Objectives: The goal of this study is to identify the various stages in liver diseases employing pyRadiomics features by analyzing the 3-dimensional CT and US images. **Methods:** The study uses Gray level Run Length Matrix for feature extraction and 3D-CNN for classification and compared with methods like Support Vector Machine (SVM), Random Forest (RF), and Naïve Bayes (NB) classifiers to assess the efficiency of the proposed model. The suggested algorithm is implemented using the library functions in Tensorflow and Keras packages in Python. **Findings:** The study utilizes radiomic feature extraction and two-phase classification to detect and classify liver disorders. In the first phase, binary classification is used to classify US and CT images as normal or abnormal, with accuracy rates of 95.4% and 97.9%. This is followed by the second phase classification, which classifies the lesion stages for both US and CT aberrant images. CT images have been shown to be more accurate in categorizing lesion stages than US imaging. CT images have a much lower misclassification rate at each step than US images. Finally, the effectiveness of the 3D-CNN model is compared with SVM, RF, and NB and the suggested method outperforms the other methods. **Novelty:** The suggested architecture employs radionics feature extraction with two-phase CNN for classification and the suggested method is found to be more efficient than SVM, RF, and NB.

Keywords: Radiomics; Feature Extraction; Convolutional Neural Networks (CNN); Classification; Liver Diseases

1 Introduction

Liver lesions are abnormal development in the liver. Liver lesions are observed in up to 30% of adults over the age of 40. Early detection and exact diagnosis of focal liver lesions (FLLs) is essential for subsequent proper treatment. The imaging techniques such as Ultrasound (US), Computed Tomography (CT), and magnetic resonance imaging (MRI) are used as noninvasive methods in medical image processing to classify

and predict liver lesions. Deep learning approaches, particularly CNN, have resulted in exceptional results on a wide range of applications, including speech recognition, recognition, and classification of images and using huge-scale datasets with annotations.

The classification is performed in two phases. In the first phase, normal or abnormal image classification is carried out using 3D CNN. If the image is abnormal then the lesion region is separated by employing a random forest algorithm since it gives prominent results in the segmentation process. The features of the segmented lesion region are extracted with the help of the Gray Level Run-Length Matrix (GLRLM). This is implemented using pyRadiomics of Python which is an inbuilt package that gives all the texture features needed for the classification process

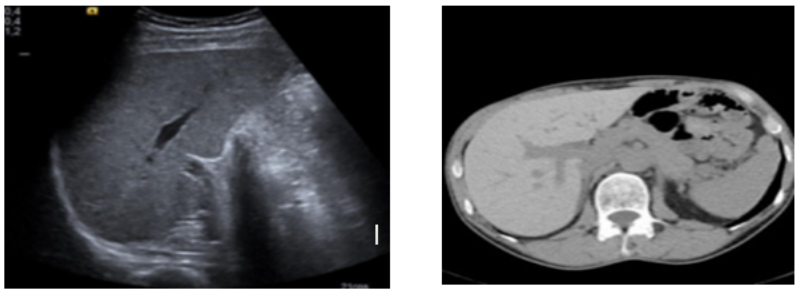

Fig 1. a) Liver Image-3D-US, b) Liver Image-3D-CT

In the second phase of classification, the 3D CNN model predicts the stages of the liver lesion using GLRLM features from pyRadiomics. The lesion is classified into four stages: the first stage is fatty liver, the second stage is compensated cirrhosis, the third stage is decompensated cirrhosis and the final stage is hepatocellular carcinoma. The model is applied for both CT and US image sets and the result is compared.

PyRadiomics was used by Tharmaseelan et.al in [1] to derive radio mic characteristics from each lesion. The performance of multiple radiomics-based machine-learning classifiers for lesions was explored and compared with an image-based DL approach utilizing a DenseNet-121. CT-based radiomics and DL allow differentiation between the causes of metastases to the liver and gastrointestinal cancers. In contrast to DL, radiomics-based models demonstrated variable generalization in discriminating liver metastases from colorectal cancer and pancreatic adenocarcinoma.

Clinically-inspired features that reflect the patient's characteristics which are often investigated by experienced radiologists during the screening process. Such features are coupled with the radiomic ones extracted from the liver, and from the suggested region of interest which captures the liver's boundary. The rigorous experiments, performed over two heterogeneous clinical datasets (two cohorts of 241 and 32 patients) revealed that extracting radiomic features from the liver's rectified contour is pivotal to enhancing the classification abilities of the supervised learners [2]. The goal of the work by Zhaoyu et.al in [3] is to create models for the various stages of Schistosoma-induced liver fibrosis using ultrasound radiomics and Machine Learning approaches. The most significant radiomic features were retrieved using PyRadiomics. Support Vector Machine (SVM) was used to build ML models and the contribution of various attributes to the model was characterized using Shapley Additive Explanations (SHAP). It is found that ML models based on ultrasound radiomics are capable of identifying various stages of liver fibrosis resulting from Schistosoma infection.

Cai et.al designed an intelligent artificial intelligence (AI)-an assisted model that uses ultrasound and radiomics flow to distinguish between different forms of Hepatic echinococcosis (HE). The study in [4] uses ultrasonography-based radiomics methods to build ML and DL models for the classification of HE. The ML models are based on eight classifiers: SVM, auto-encoder (AE), linear discriminant analysis, random forest (RF), logistic regression, adaptive boosting, decision tree, and Naive Bayes models. The use of an AI-assisted approach could improve ultrasonic diagnostic abilities and help with the classification of HE in high-endemic locations.

Radiomics promises to improve hepatocellular carcinoma (HCC) diagnosis and prognosis by utilizing AI algorithms to extract vast amounts of information from medical images. Radiomics generates a set of iconic and reliable imaging characteristics that are linked to major clinical or genetic biomarkers, allowing HCC patients to be risk-stratified before surgery. In addition to outcome data, a complete mix of radiomic, clinical, and/or multiomics data may improve direct prediction of therapy response and prognosis. The advancement of radiomics is transforming our knowledge of individualized precision medicine in HCC treatment [5,6]. The study by Zhang et.al in [7] extracts CT radiomics features to categorize the gross tumor volume and normal liver tissue in hepatocellular carcinoma using common ML methods, with the goal of creating a computer-

based classifier model. Radiomics algorithms were developed using LR, SVM, RF, XGboost, and Adaboost algorithms. CT radiomics based on ML algorithms can properly differentiate between Gross Tumor Volume (GTV) and normal liver tissue, with the XGboost and SVM algorithms serving as the most effective complementing algorithms.

A deep learning radiomics (DLR) algorithm created by Jia W et.al in [8] using contrast-enhanced CT was used to determine the major source of liver metastases. It is developed to distinguish between the five pathogenic forms of liver metastases. The algorithm's classifying efficiency was improved by using progressive classification. Lesions were initially divided into digestive tract cancer (DTC) and non-digestive tract cancer (non-DTC). The DLR model is an excellent tool for determining the primary cause of liver metastasis. Mitrea et.al [9] created image analysis and identification algorithms for automatic and computer-aided diagnosis of HCC. Our research included conventional approaches that combined advanced texture analysis, primarily based on Generalized Co-occurrence Matrices (GCM), with traditional classifiers, as well as deep learning approaches based on Convolutional Neural Networks (CNN) and Stacked Denoising Autoencoders (SAE) and attained the highest accuracy of 91% for B-mode ultrasound pictures using CNN.

With massive volumes of quantitative health care record information and imaging characteristics, experts have utilized image-based approaches like radiomics and AI to automatically acquire and analyze multidimensional data from images. The combination of these data can yield clinically useful results that can be used to drive tailored treatment regimens and maximize resource utilization. Hsieh et.al in [10] explains the fundamentals of machine learning and provides an in-depth investigation into predicting response to treatment in HCC patients following less-invasive image-guided treatment.

The objective of the review by Maino C et.al in [11] is to highlight the most pertinent and robust research reported in the field of liver radiomics, identifying their main constraints and concerns, as well as what they can contribute to the future of medical practice and research.

The fetal lungs and liver damaged by CDH were automatically contoured on MRI sections by the study in [12], which used a publicly available deep learning (DL) segmentation system (nnU-Net). Subsequently, both manually and automatically segmented regions had their standard features from pyRadiomics obtained. The Wilcoxon rank-sum test and intraclass correlation coefficients (ICCs) were used to assess the consistency of features between the two groups. Finally, built an ML classifier system for liver herniation prediction based on SVM and trained on shape data computed in both the traditional and nnU-Net-segmented organs. This allowed researchers to evaluate the reliability of the automatic-segmentation strategy. The severity of liver cirrhosis may be predicted by MRI-based radiomics characteristics of the liver and spleen, with dispensation or MELD status serving as a crude proxy for disease severity [13]. Table 1 lists the recent studies in the literature to predict lesions in livers using radiomics features and ML methods.

Table 1. Recent studies about the Radiomics features for lesion identification

Authors/ Year	Method	Pros	Cons
Tharmaseelan et al., 2023 [1]	KNN and image-based DenseNet-121-classifier	The performance of radiomics-based models to discriminate between pancreatic adenocarcinoma and colorectal cancer and liver metastases varied.	restricted to a tiny, homogeneous patient group with similar scan settings
Kotowski et al.,2023 [2]	Radiomic Features	Handles heterogeneous data enhance feature interpretability	Time consuming and user dependent process
Gu et al.,2023 [3]	Mann-Whitney U test, and LASSO, SVM and SHAP	It is possible to classify the various stages of liver fibrosis brought on by Schistosoma infection using ML models based on ultrasound radiomics.	Lasso is not suited for datasets containing correlated features
Cai R et al., 2024 [4]	SVM, AE, linear discriminant, RF LR, adaptive Boosting , NB n EfficientNetB0, InceptionV3, ResNet50 and VGG19,	Improve diagnostic accuracy in the basic medical settings	Fails to integrate clinical information
Prior et al., 2024 [6]	Unsupervised Learning	Identified on CT scans, allowing stable tumor habitat modeling to quantify tumor heterogeneity.	Limited pattern discovery and interpretability.
Zhang et al.,2024 [7]	LASSO regression. LR, SVM, RF, Adaboost and XGBoost	Accurately classify the gross tumour volume(GRV) and normal tissue liver.	Biased and instability

Continued on next page

Table 1 continued

Jia w et al., 2024 [8]	DLR model	In both the external test set and validation set, radiomics characteristics demonstrated the best discrimination	The networks typically require more data to identify predicted patterns because they are not provided with predefined features.
Mitrea et al., 2023 [9]	GCM, CNN, SAE	Combines the benefits of both Conventional and DL approaches	More complex
Hsieh et al.,2023 [10]	Radiomics and AI	managing enormous volumes of data in contrast to traditional statistics	Complex processing
Conte et al., 2024 [12]	SVM and nnUNet	Automatic segmentation, feasible and offers good reliability	SVM take larger training time and difficult to choose a kernel function
Nitsch et al., 2021 [13]	Radiomic Feature Analysis, Cross Validation , RF	Stable and Generalized	Precise prediction needs more trees resulting in slower model
Cao et al., 2024 [14]	TSETMF	Better denoising stability and less decrease in PSNR	Fails to capture all the information

Radiomics should be viewed as a useful technique in liver disorders. It can aid in the diagnosis of fatty liver disease, inflammatory processes, and stage fibrosis, exceeding clinical indices. It also improves the identification, staging, and prognosis of HCC. It can be used to treat liver metastases, particularly colorectal cancer. From the literature study, it is found that the radiomics feature extraction is vital for the detection of liver diseases of various types. Furthermore, the ML methods are used in the classification of the disease based on the features. The present study employs the Radiomics feature extraction, followed by CNN classification in order to predict liver diseases efficiently. Developments in ML can help clinicians to analyze and assess liver diseases using US and CT images in entirely novel ways. The objective of the study is:

- To study the role of radiomics in the detection of liver diseases
- To design an architecture for feature extraction and classification from the US and CT images.
- To assess the performance of the algorithms using performance metrics

The paper is structured as follows. The section provides a brief note on the liver lesions and the radiomics features that aid in the prediction of liver diseases using ML methods followed by the related works. Section 2 offers the methodologies used in the study followed by results and discussions in section 3. Section 4 concludes the study with the future scope.

2 Methodology

The model architecture depicted in Figure 2 comprises preprocessing and extracting the features in the liver from the dataset and employs the 3D-CNN model to classify it as normal or abnormal images. If abnormal, liver lesions are segmented using the Random Forest (RF) model, and the radiomics features are extracted using GLRLM from the segmented image. Again the 3D CNN is employed to classify it further as fatty liver (FL), Compensated Cirrhosis (CC), Decompensated cirrhosis (DC), and Hepatocellular carcinoma (HCC).

In the preprocessing, a 3D median filter is employed and the noises are removed. 3*3*3 filters are used to sharpen the image. The edge feature that belongs to the image is well preserved compared to other filters like mean and Gaussian where little blur of the edges occurs. In the case of the filter window that lays over an edge, the median filter will not generate new nonrealistic pixel values, the edge information is preserved. Using this method, the pixel that contains all the distribution values of intensity will be assigned a median value, and a new image will be formed that matches the original [14].

The liver segmentation is performed by employing watershed algorithms. Voxels that have greater value will combine with seeds. The region is growing in both the temporal and special directions. The 3D watershed exhibits a surface composed of pixels that form a boundary of a region. Figure 6 presents the segmented liver of CT and US images for further processing.

Figure 3**(a)**and **(b)** show the noisy images of CT and US **(b)** and **(d)** show the images of CT and US respectively after the removal of noise and **(d)** and **(f)** show the segmented liver images.

In the first phase of classification, the liver is classified into normal or abnormal using the 3D-CNN model. In the CNN model, eight filters (7x7x7) are used in the first convolution layer. The number of filters is increased in the second and third layers with 16, and 32 filters, of size 5x5x5 and 3x3x3. Next to Convolution layer pooling layer is used that reduces the spatial size

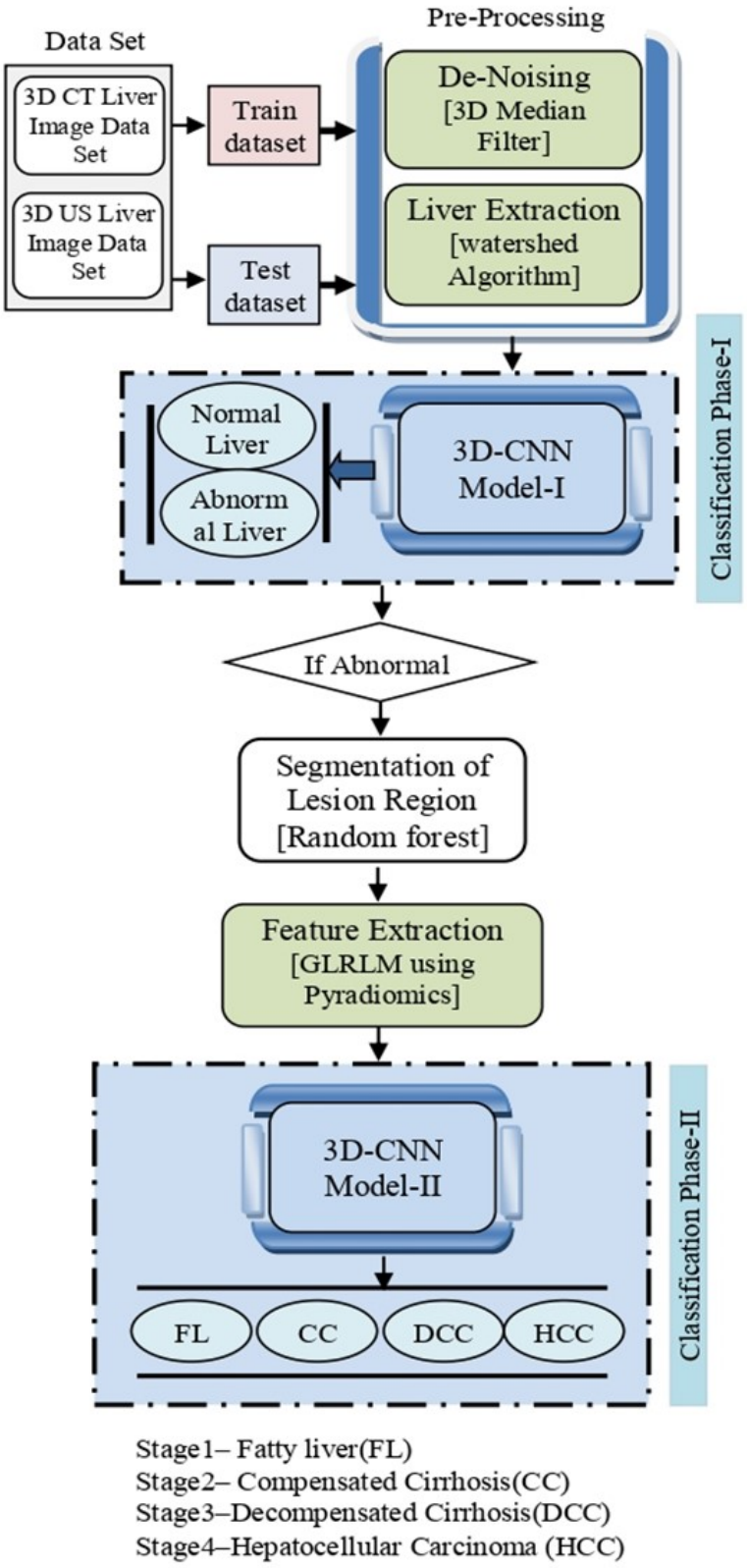

Fig 2. Proposed architecture of Feature Extraction and Classification model

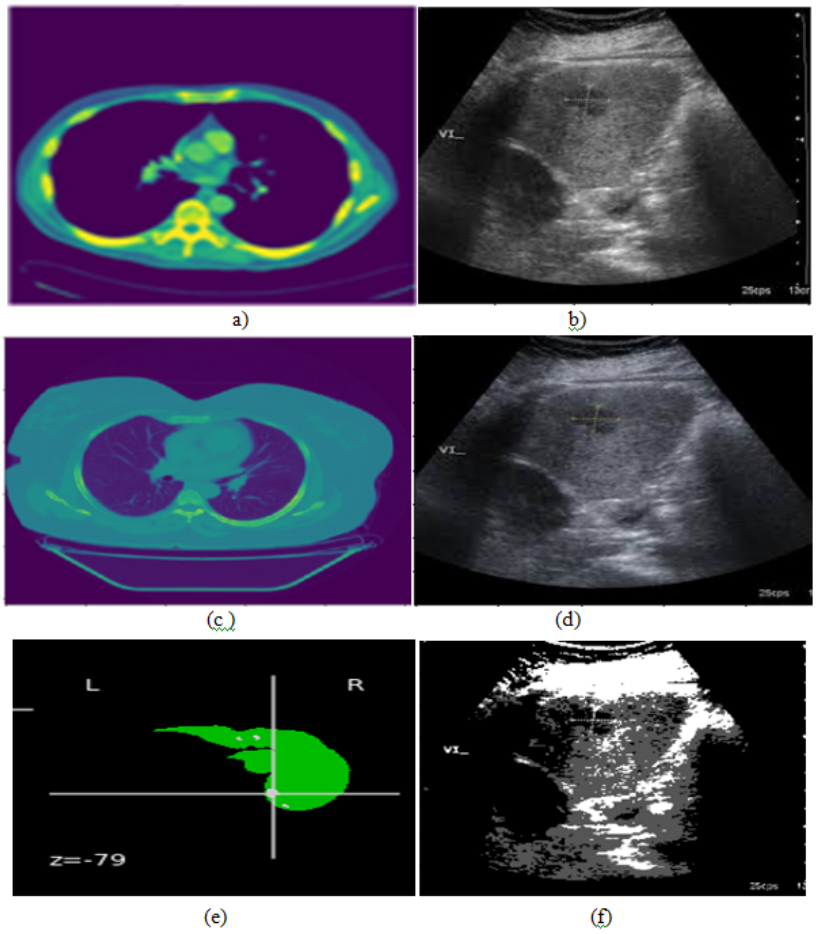

Fig 3. (a) and (b) –Noisy Liver Images (c) and (d)De-noise images (e) and (f) Segmented Liver Images of CT and US images respectively

of the features of the convolution layers. Maxpool with a kernel of 3x3x3 is used is used in this model. The activation function ReLu is included in the model. The model is executed for 50 epochs with a batch size of 20. The final layer is the fully connected layer in which the Liver abnormality is classified.

Random Forest (RF) algorithm is used to segment the lesion region implemented in Python and this algorithm gives the result based on the prediction of the decision trees. This algorithm is very suitable for mixed data (numerical and categorical data) and is able to approximate any kind of function. The extraction of radiomics features is then performed using the Gray Level Run Length Matrix (GLRLM). pyRadiomics, the open-source package in Python, is used to extract the features of 3D images. SimpleITK of Python is used to load the image data. The gray-value runs are calculated by finding the number of voxels between successive voxels with equal gray values. The run length-encoding for orientations (0°, 45°, 90°, and 135°) produces a run length matrix. Table 2 lists the GLRLM features and the corresponding gray values.

Table 2. GLRLM Features

GLRLM Features	Gray Values
GrayLevelNon-Uniformity	175.6351923150419
GrayLevelNon-UniformityNormalized	0.04514123814981055
GrayLevelVariance	39.118151021979244
HighGrayLevelRunEmphasis	281.066493908972
LongRunEmphasis	1.2268440382584342
LongRunHighGrayLevelEmphasis	341.2865790983503
LongRunLowGrayLevelEmphasis	0.010601170478748765

Continued on next page

Table 2 continued

LowGrayLevelRunEmphasis	0.008600397891661503
RunEntropy	4.915038003159503
Run LengthNon-Uniformity	3500.0432315746298
RunLengthNon-UniformityNormalized	0.8950494659480998
RunPercentage	0.9404064632491029
RunVariance	0.08479457789590625
ShortRunEmphasis	0.9559391731405504
ShortRunHighGrayLevel Emphasis	268.9741798411307
ShortRunLowGrayLevelEmphasis	0.008229766244155428

In the first phase, the normal and abnormal images(segmented) are classified. In the second phase of classification, the segmented abnormal image is again classified into four stages. The four output nodes formed in the output layer help to classify the Lesion stages as shown in Figure 4**(a)** shows the fatty liver with liver cirrhosis, **(b)** depicts the compensated image and **(c)** shows the decompensate images.

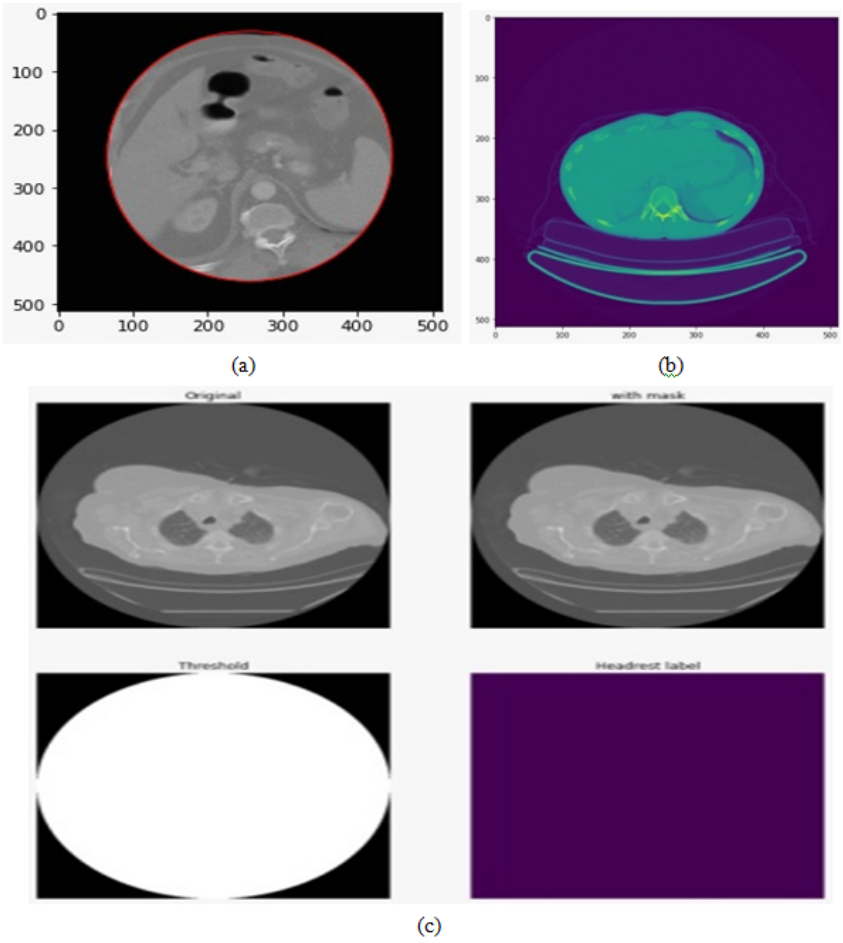

Fig 4. (a) Fatty Liver–ChronicHepatitis, b) Compensated cirrhosis, c) Decompensated Cirrhosis

The dataset contains 800 CT images and 800 US images in DICOM format. The dataset is split as a training set and testing set in the ratio 70:30. In this there are 560 trained images and 240 test images for both CT and US individually. An example dataset images are shown in Figure 5 and the number of images considered for training and testing is shown in Table 3. The dataset contains four categories of images: 1-fatty liver (FL), 2-compensated Cirrhosis (CC), 3-Decompensated Cirrhosis (DCC), 4-Hepatocellular Carcinoma (HCC) and normal liver images. The images are split up into normal and abnormal.

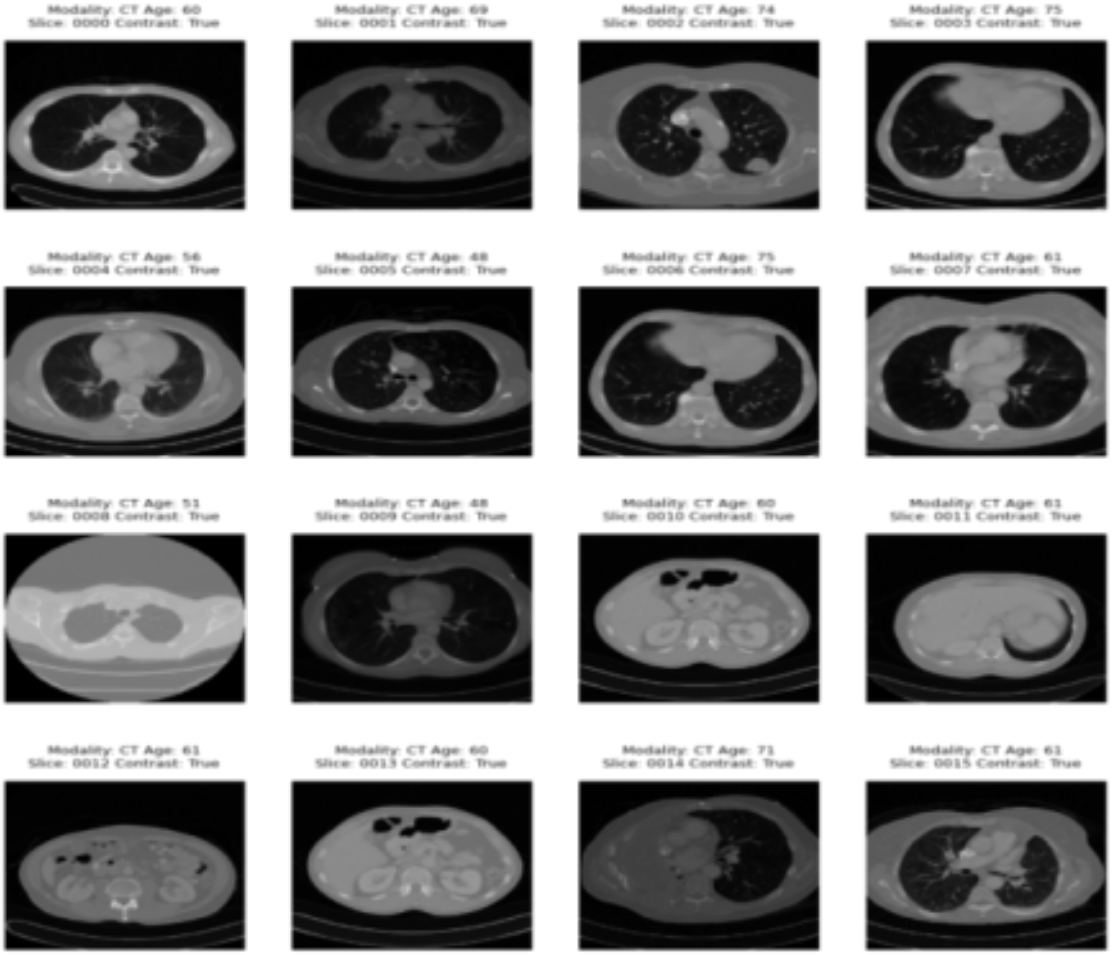

Fig 5. Dataset Sample Liver Images

Table 3. 3 Dataset Split-up – Training set and Testing set

Phase-I	**US Images**		**CT Images**	
	Train set	**Test Set**	**Train set**	**Test Set**
Normal	100	40	80	40
Abnormal	460	200	480	200
Total	560	240	560	240
Lesion Stages	**Ground Truth of Abnormal Images**			
	US Images		**CT Images**	
	Train set	**Test set**	**Train set**	**Test set**
FL	80	30	75	30
CC	100	45	110	45
DCC	120	55	125	55
Total	460	200	480	200

3 Results and Discussion

In Classification Phase-I 240 test images of US and CT are tested with the trained 3DCNN model-I. This model is trained to classify Normal or abnormal images. For US images, this model correctly predicts 194 abnormal images and 35 normal images. Eleven images have been misclassified in which 6 abnormal images are misclassified as normal images and 5 normal images as abnormal images. The confusion matrix for 3D CNN models using US and CT images is shown in Figure 6**(a)** and **(b)** respectively. In the confusion matrix, N indicates 'Normal' and AB indicates 'Abnormal'. Similarly, For CT images, the model correctly predicts 197 abnormal images and 38 normal images. Five images have been misclassified which 3 abnormal images are misclassified as normal images and 2 normal images as abnormal images.

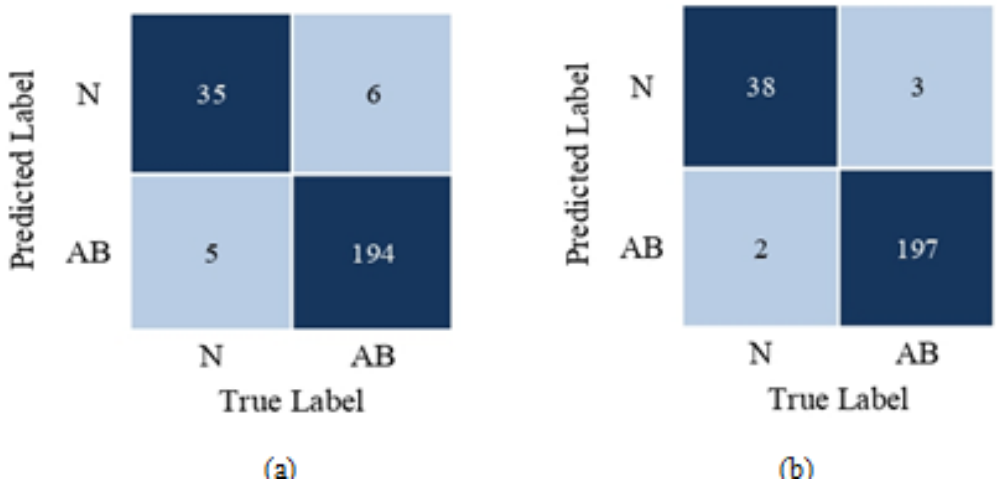

Fig 6. Confusion Matrix for Phase-I Classification (a) US and (b) CT images

Test set accuracy in the classification of Normal or abnormal images for US Images = (35+194)/240= 95.4%

Test set accuracy in the classification of Normal or abnormal images for CT Images = (38+197)/240= 97.9%

In Classification Phase II 200 abnormal images have been taken as test images of US and CT which are tested with the trained 3DCNN model-II. This model is trained to classify Lesion stages. For US images, this model correctly predicts 187 images. 13 images have been misclassified. The confusion matrix for the 3D CNN model using US and CT images is given in Figure 7. The Confusion Matrix for the US image is a 4x4 matrix for fatty liver, 2 images are misclassified as CR and DCR. For CC 4 misclassification occurs where 2 is FL, 1 is DCR and 1 is HCC. Similarly, for DCC, 3 misclassifications, and HCC, 4 misclassifications occur.

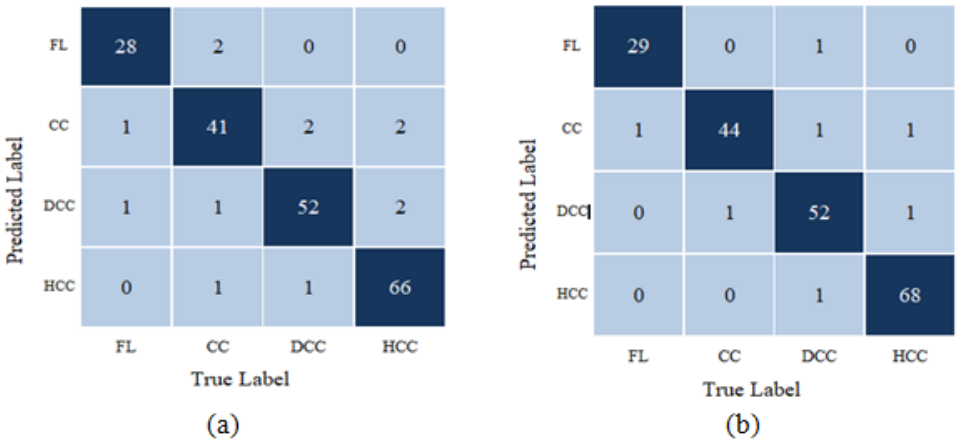

Fig 7. Confusion Matrix for Phase-II Classification (a)US and (b)CT images

Table 4. Prediction Analysis – US and CT Images

Stages	US Images			CT Images		
	No. of samples Input	Correct Prediction	Wrong Prediction	No. of samples Input	Correct Prediction	Wrong Prediction
FL	30	28	2	30	29	1
CC	45	41	4	45	44	1
DCC	55	52	3	55	52	3
HCC	70	66	4	70	68	2
Total	200	187	13	200	193	7

Test set accuracy in lesion stage classification of US Images = (28+41+52+66)/200= 93.5%

Test set accuracy in lesion stage classification of CT Images = (29+44+52+68)/200= 96.5%.

From Table 4, it is evident that the prediction accuracy for US images is higher than for the CT images. Even though it varies between the two modalities, the 3D-CNN model performs better than the other state-of-the-art methods for both US and CT images. This study emphasizes the design of a new model to generalize the classifier for all the image modalities.

Table 5. Misclassification Analysis

Stages	Accuracy in Percentage		Misclassification Rate in percentage	
	Abnormal US Images	Abnormal CT images	For US Images	For CT Images
FL	93.333	96.666	0.0714	0.0333
CC	91.111	97.777	0.0888	0.0222
DCC	94.545	94.545	0.0545	0.0545
HCC	94.285	97.142	0.0571	0.0286

Similarly, from Table 5, it is observed that the misclassification rate for CC (compensated Cirrhosis) is very high for US images and less for CT images. It is also observed that the misclassification rate for a certain stage (CC) of liver diseases is high compared to the other stages (FL, DCC, HCC).

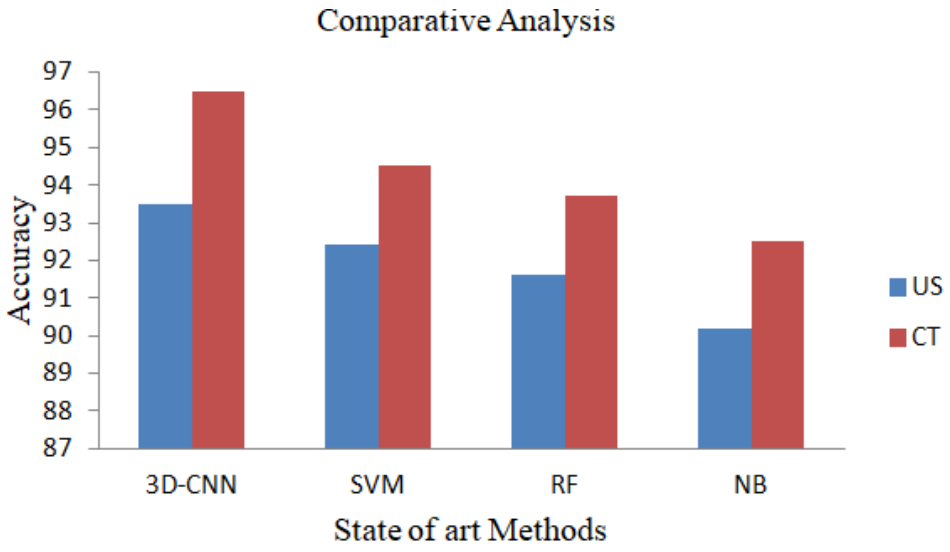

Fig 8. Accuracy Analysis Proposed and State-of-art Methods

The proposed 3D-CNN is compared with the SVM, RF, and NB methods. It is found from Figure 8, that the accuracy is high and the misclassification rate is low in the case of 3D-CNN models. Since it involves two phases of classification, the performance of the suggested 3D-CNN is high for the stages of liver cirrhosis. The SVM, RF, and NB are in the next decreasing order of performance for the same set of US and CT images.

4 Conclusion

The study employs radiomics feature extraction and two-phase classification for the detection and classification of liver diseases. In the first phase, binary classification is performed where the US and CT images are classified into normal or abnormal images with an accuracy of 95.4% and 97.9%. This is followed by the second Phase classification where the lesion stages are classified for US as well as CT abnormal images. It is observed that using CT images is effective in classifying the lesion stages compared to US images with more accuracy. The misclassification rate for each stage is very low for CT images compared to US images. The proposed 3D-CNN is compared with the state of art methods like SVM, RF, and NB to study the effectiveness of the suggested methods. It is found that the prediction accuracy is more in the case of the suggested methods than the other methods used for comparison. The study can be further extended to classify more categories of liver diseases and also can be employed to identify other diseases. Further, the study can be extended to create a classifier model that works well for all image modalities like MRI and other liver screening devices.

References

1) Tharmaseelan H, Vellala AK, Hertel A, Tollens F, Rotkopf LT, Rink J, et al. Tumor classification of gastrointestinal liver metastases using CT-based radiomics and deep learning. . *Cancer Imaging*. 2023;23:95–95. Available from: https://doi.org/10.1186/s40644-023-00612-4.
2) Kotowski K, Kucharski D, Machura B, Adamski S, Becker BG, Krason A, et al. Detecting liver cirrhosis in computed tomography scans using clinically-inspired and radiomic features. . *Computers in biology and medicine*. 2023;152:106378–106378. Available from: https://doi.org/10.1016/j.compbiomed.2022.106378.
3) Guo Z, Zhao M, Liu Z, Zheng J, Gong Y, Huang L, et al. Feasibility of ultrasound radiomics based models for classification of liver fibrosis due to Schistosoma japonicum infection. . *PLOS Neglected Tropical Diseases*. 2024;18:12235–12235. Available from: https://doi.org/10.1371/journal.pntd.0012235.
4) Cai D, Zhang X, Suolang L, Ren Y, Wang Y, Zhong X, et al. Classification of hepatic echinococcosis based on ultrasound using radiomics approaches including machine large-scale, dual-center application study. *Research Square*. Available from: https://doi.org/10.21203/rs.3.rs-4370729/v1.
5) Berbís MA, Godino FP, Rodríguez-Comas J, Nava E, García-Figueiras R, Baleato-González S, et al. Radiomics in CT and MR imaging of the liver and pancreas: tools with potential for clinical application. . *Abdominal Radiology*. 2024;49:322–362. Available from: https://doi.org/10.1007/s00261-023-04071-0.
6) Prior O, Macarro C, Navarro V, Monreal C, Ligero M, Garcia-Ruiz A, et al. Identification of precise 3D CT radiomics for habitat computation by machine learning in cancer. *Radiology: Artificial Intelligence*. 2024;6(2). Available from: https://doi.org/10.1148/ryai.230118.
7) Zhang HW, Huang DL, Wang YR, Zhong HS, Pang HW. CT radiomics based on different machine learning models for classifying gross tumor volume and normal liver tissue in hepatocellular carcinoma. *Cancer Imaging*. 2024;24:20–20. Available from: https://doi.org/10.1186/s40644-024-00652-4.
8) Jia W, Li F, Cui Y, Wang Y, Dai Z, Yan Q, et al. Deep Learning Radiomics Model of Contrast-Enhanced CT for Differentiating the Primary Source of Liver Metastases. . *Academic Radiology*. 2024. Available from: https://doi.org/10.1016/j.acra.2024.04.012.
9) Mitrea D, Brehar R, Nedevschi S, Lupsor-Platon M, Socaciu M, Badea R. Hepatocellular Carcinoma Recognition from Ultrasound Images Using Combinations of Conventional and Deep Learning Techniques. *Sensors*. 2023;23(5):2520–2520. Available from: https://doi.org/10.3390/s23052520.
10) Hsieh C, Laguna A, Ikeda I, Maxwell AW, Chapiro J, Nadolski G, et al. Using machine learning to predict response to image-guided therapies for hepatocellular carcinoma. *Radiology*. 2023;309(2):222891–222891. Available from: https://doi.org/10.1148/radiol.222891.
11) Maino C, Vernuccio F, Cannella R, Franco PN, Giannini V, Dezio M, et al. Radiomics and liver: Where we are and where we are headed? *European Journal of Radiology*. 2024;p. 111297–111297. Available from: https://doi.org/10.1016/j.ejrad.2024.111297.
12) Conte L, Amodeo I, De Nunzio G. Congenital diaphragmatic hernia: automatic lung and liver MRI segmentation with nnU-Net, reproducibility of pyRadiomics features, and a machine learning application for the classification of liver herniation. *Eur J Pediatr*. 2024;183:2285–2300. Available from: https://doi.org/10.1007/s00431-024-05476-9.
13) Nitsch J, Sack J, Halle MW. MRI-based radiomic feature analysis of end-stage liver disease for severity stratification. *Int J CARS*. 2021;16:457–466. Available from: https://doi.org/10.1007/s11548-020-02295.
14) Cao N, Liu Y. High-noise grayscale image denoising using an improved median filter for the adaptive selection of a threshold. . *Applied Sciences*. 2024;14:635–635. Available from: https://doi.org/10.3390/app14020635.